

What smooth surfaces can be constructed from total degree 2 splines?

Jörg Peters¹, Kęstutis Karčiauskas

Abstract

On a planar Euclidean domain, Powell-Sabin splines form a rich space of C^1 polynomials of total degree 2, i.e. with constant second derivatives. However, when the domain has a different structure because the genus of the surface is not 1, building curved free-form surfaces solely with total degree quadratic polynomials, with each piece defined over a flat, straight-edge domain triangle, meets with obstructions. By pinpointing these obstructions, the limitations of modeling with quadratics are made precise, the allowable C^1 free-form constructions are characterized and their necessary shape-deficiency is demonstrated.

Keywords: G^1 spline, total degree 2, Powell-Sabin, Zwart-Powell, rational spline

1. Introduction

Total-degree 2 (quadratic) polynomial pieces offer exact-parametrizable planar slices, as conics, and hence exact tracing of level curves that avoids numerical ambiguity, say in the occlusion due to multiple silhouette curves in Capouellez et al. (2023). The Powell-Sabin (PS) spline construction of Powell and Sabin (1977) generate smoothly-joined pieces of total degree 2 and is commonly used to model graphs of functions, e.g. for scattered data fitting, see Dierckx et al. (1992); Dierckx (1997); Manni and Sablonniere (2007). The spline space affords local subdivision Speleers et al. (2006), a B-spline-like basis Cohen et al. (2013); Windmolders and Dierckx (1999, 2000); Speleers et al. (2007, 2012, 2013); Beirão da Veiga et al. (2015) and generalizes to higher degree and smoothness Lyche and Muntingh (2019), using a 12-split of each domain triangle, see Fig. 1 and Alfeld et al. (1996a).

Both the Powell-Sabin (PS) construction(s) and the bivariate 4-direction box spline, see De Boor et al. (2013); Kim and Peters (2024), also known as Zwart-Powell (ZP) element, see Zwart (1973), rely on special quadrilateral configurations in the domain partition, the yellow-tinged regions in Fig. 1 and Fig. 2. Given any four points in \mathbb{R}^n , in Fig. 2 displayed as 4a, 4b, 4c, 4d with the factor 4 explicitly pulled out for subsequent averaging, we observe that the average of the horizontal averages, $2(d+a)$ and $2(b+c)$, equals the the average of the vertical averages $2(a+b)$ and $2(c+d)$, Fig. 2 a. The averages all lie in one plane, the tangent plane of the patches meeting at the shared vertex $a+b+c+d$ where they share the normal direction $(c+d-a-b) \times (a+d-c-d)$.

For polynomials of total degree, over triangular domains, these special configurations are sometimes called degenerate but they are not singularities. Rather, the configuration simplifies the algebraic conditions, namely collinearity of transversal derivatives, that imply C^1 continuity across all four boundaries. Specifically, for total degree quadratic polynomials, the configurations pin down all but one free vertex per quadratic piece, namely the central points of the pink-tinged regions. For the total degree 2 constructions of Zwart (1973) and of Powell and Sabin (1977), the coefficients in the pink-tinged regions automatically form and lie in a shared (tangent) plane. For the PS construction,

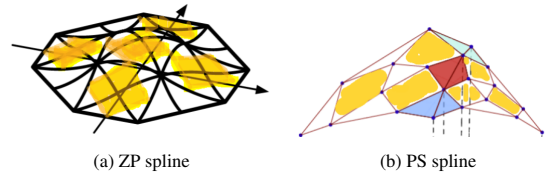


Figure 1: Piecewise quadratic B-spline-like constructions: images adapted (a) from Kim and Peters (2024), (b) from Cohen et al. (2013)

Email addresses: jorg.peters@gmail.com (Jörg Peters), kestutis.karciauskas@mif.vu.lt (Kęstutis Karčiauskas)

this follows from the fact that any three points lie in a plane and the remaining coefficients are their averages. The ZP construction explicitly places all four corners of each pink-tinged quadrilateral region in a plane in Fig. 2 b,c; the remaining pink-underlaid points are averages of these corners, so that all points lie in one plane.

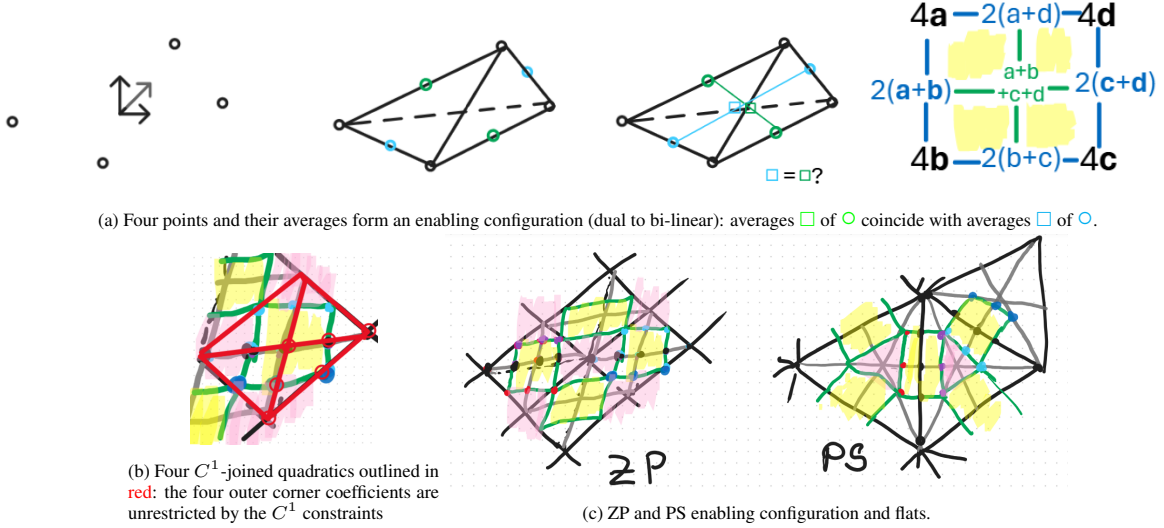


Figure 2: Yellow underlaid enabling configurations (dual of bi-linear) and pink underlaid tangent plane (flat) configurations.

The goal of this paper is to clarify whether and how smooth quadratic free-form spline surfaces can be constructed by leveraging these or similar configurations; and to examine the nuances of the claim that 'quadratic patches are capable of producing smooth spline surfaces representing general free-form shapes' (Bastl et al., 2008, p198). That is, we ask

1. Can Powell-Sabin (PS) or Zwart-Powell (ZP) constructions model smooth general free-form surfaces?
2. Can total degree 2 pieces (quadratics) model smooth general free-form surfaces? If so, how?

That is, we ask for the existence, and, if true, for in a concrete, preferably local, construction. Much depends on the **Assumptions**: We assume that the degree 2 splines are piecewise represented over

- domain triangles that are flat and have straight edges and
- that a smooth join between the pieces is characterized by Lemma 1.

Lemma 1 (G^1 constraints, DeRose (1990); Peters (1990)). Two polynomial pieces $\mathbf{p}, \mathbf{q} : (u, v) \rightarrow \mathbb{R}^3$ join G^1 along the common boundary $\mathbf{p}(u, 0) = \mathbf{q}(u, 0), u \in [0..1]$ if and only if there exist polynomials $\lambda, \mu, \nu : [0..1] \rightarrow \mathbb{R}, \mu\nu > 0$, so that

$$\lambda(u) \partial_u \mathbf{p}(u, 0) = \mu(u) \partial_v \mathbf{p}(u, 0) + \nu(u) \partial_v \mathbf{q}(u, 0), \quad u \in [0..1]. \quad (\text{G1})$$

(G1) can be derived by expanding $\partial_v(\mathbf{q} - \mathbf{p} \circ \rho)(u, 0) \equiv 0$, where the gradient of the re-parameterization ρ equals $[\lambda(u)/\nu(u), \mu(u)/\nu(u)]^t$ with λ, μ, ν polynomial (up to a common factor) since $\partial_u \mathbf{p}$, $\partial_v \mathbf{p}$ and $\partial_v \mathbf{q}$ are polynomials. We have the following reparameterization degree bounds.

Lemma 2. (Peters, 1990, Corollary 2.5) If, in Lemma 1, \mathbf{p}, \mathbf{q} are non-singular, of total degree 2 and λ, μ, ν do not share a common factor then λ, μ, ν are each of degree at most 2.

Along the boundary, the first partial derivatives, i.e. the tangents of the G^1 -joined pair \mathbf{p}, \mathbf{q} are related by a *single affine* map if and only if λ, μ and ν are all constant. If λ, μ and ν are all constant then a piecewise affine map can embed the domains, both of \mathbf{p} and \mathbf{q} , into \mathbb{R}^2 . And since every point on a G^1 surface has a well-defined tangent plane that the tangents of the patch-separating curves split into sectors whose opening angles sum to 2π , the domain pieces of the pre-image can be joined so their angles sum to 2π .

Observation 1. *Given a point on the G^1 surface surrounded without gap or overlap by surface pieces \mathbf{p}^i , $i = 1, \dots, n$. If, for each pair $\mathbf{p}^i, \mathbf{p}^{i+1}$, the reparameterization is a single affine map then the domains of the \mathbf{p}^i can be piecewise-affinely embedded into \mathbb{R}^2 to surround the pre-image of the point without gap and overlap.*

Overview An example in Section 2 shows that the direct use of the Powell-Sabin approach fails to generate a piecewise quadratic smooth surface already for an octahedral input triangulation. Section 3 establishes the shape restrictions when modeling with piecewise quadratic polynomials. Section 4 lists smooth quadratic spline constructions that obey those shape restrictions or side-step the assumptions.

2. A symmetric counterexample to free-form Powell-Sabin constructions

This section shows and discusses how the [Powell and Sabin \(1977\)](#) construction fails to generate a closed piecewise quadratic smooth surface for the octahedron triangulation. The Powell-Sabin spline is a piecewise total degree 2 C^1 function on a triangulation of \mathbb{R}^2 . Each triangle is covered by a macro-patch consisting of six quadratic pieces whose domains are delineated by the PS-split of the domain triangle, see Fig. 3 b.

Definition 1 (PS-split, label/index conventions, Greville abscissae). *For the PS-split of a triangle, we join the centers, labeled 00, of adjacent triangles (labeled oab and obc in Fig. 3 a) by a straight line segment (that intersects the line segment ob) and additionally join each center by a straight line segments to each of the corner vertices (with index 02) of the triangle. This splits each macro-triangle into 6 sub-triangles. The Greville abscissae of each sub-triangle oia are uniformly-placed at $(ia + jb + ko)/2$, where $i + j + k = 2$ and i, j, k are non-negative integers.*

Fig. 3 b shows the PS split of the macro-triangle into six sub-triangles, each to be covered by a quadratic piece. The degree 2 pieces can conveniently be expressed in terms of Bernstein polynomials $i, j, k \in \mathbb{N}_0$

$$B_{ijk}(u, v) := \binom{2!}{i!j!k!} w^k u^i v^j, \quad i + j + k = 2, \quad 0 \leq u, v, w, u + v + w = 1.$$

Then the total degree 2 Bernstein-Bézier form (BB-form, [de Boor \(1987\)](#); [Farin \(1988\)](#); [Prautzsch et al. \(2002\)](#)) of each polynomial piece is $\mathbf{p}(u, v) := \sum_{i+j+k=2} \mathbf{p}_{ij} B_{ijk}(u, v)$ and the \mathbf{p}_{ij} are the BB-coefficients. The indices (subscripts, ij , $i + j \leq 2$, dispensing with the $k = 2 - i - j$), associated with the Greville abscissae, and the labels (superscripts such as *oba*) of the BB-coefficients of one degree 2 piece, associated with the sub-triangles, are illustrated in Fig. 3 a. The two sub-triangles attached to *o*, of the triangle *oab*, have BB-coefficients \mathbf{p}_{ij}^{oba} and \mathbf{p}_{ij}^{oba} , respectively and share the common quadratic boundary curve segment with BB-coefficients $\mathbf{p}_{0j}^{oba} = \mathbf{p}_{0j}^{oba}$, $j = 0, 1, 2$. Analogously, $\mathbf{p}_{i0}^{oba} = \mathbf{p}_{i0}^{oba}$, $i = 0, 1, 2$ and, for a neighbor triangle *obc*, $\mathbf{p}_{2-i,i}^{oba} = \mathbf{p}_{2-i,i}^{obc}$, $i = 0, 1, 2$.

The PS construction is structurally symmetric in the sense that Lemma 1 holds with

$$\partial_v \mathbf{p}(u, 0) + \partial_v \mathbf{q}(u, 0) = b(u) \partial_u \mathbf{p}(u, 0), \quad u \in [0..1], \quad b : \mathbb{R} \rightarrow \mathbb{R}. \quad (G_{sym}^1)$$

Along the boundary from \mathbf{p}_{02} to \mathbf{p}_{00} the derivatives in terms of the BB-coefficients are

$$\begin{aligned} \partial_v \mathbf{p}(u, 0) &= 2(1 - u)(\mathbf{p}_{11} - \mathbf{p}_{02}) + 2u(\mathbf{p}_{10} - \mathbf{p}_{01}), \\ \partial_v \mathbf{q}(u, 0) &= 2(1 - u)(\mathbf{q}_{11} - \mathbf{q}_{02}) + 2u(\mathbf{q}_{10} - \mathbf{q}_{01}), \\ \partial_u \mathbf{p}(u, 0) &= 2(1 - u)(\mathbf{p}_{01} - \mathbf{p}_{02}) + 2u(\mathbf{p}_{00} - \mathbf{p}_{01}). \end{aligned}$$

By comparing the polynomial degrees in G_{sym}^1 , $b(u)$ must equal some constant β and

$$\begin{bmatrix} \mathbf{p}_{11} - \mathbf{p}_{02} \\ \mathbf{p}_{10} - \mathbf{p}_{01} \end{bmatrix} + \begin{bmatrix} \mathbf{q}_{11} - \mathbf{q}_{02} \\ \mathbf{q}_{10} - \mathbf{q}_{01} \end{bmatrix} = \beta \begin{bmatrix} \mathbf{p}_{01} - \mathbf{p}_{02} \\ \mathbf{p}_{00} - \mathbf{p}_{01} \end{bmatrix}. \quad (1)$$

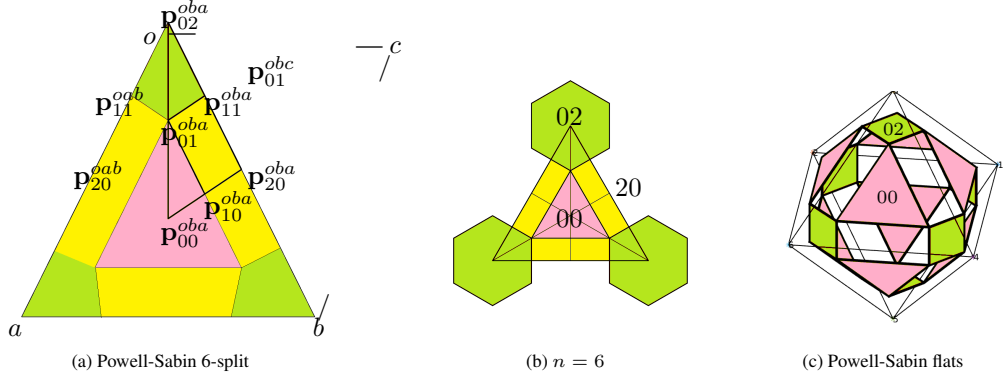


Figure 3: Powell-Sabin structure. (a) 6-split Triangle oab (neighbor triangle obc indicated by its third corner). The six BB-coefficients (of one of six quadratic patches) are indexed (by subscript) and labeled (by superscript) to be globally unique. (b) globally flat case $n = 6$ of a hex-tri mesh. (c) Collections of BB-coefficients that form tangent planes (pink, green) that must be flat on the octahedron (the yellow-tinged enabling configurations are left clear)

Lemma 3. *The Greville abscissae of the PS-split satisfy the G_{sym}^1 relations with constant $b(\cdot)$ functions.*

Proof. For each of the four abutting pairs that meet at the BB-coefficient with index 20, i.e. at the center of the enabling configuration, we have $b(u) = 0$. Along the other type of interior edge with indices 00, 01, 00, the green BB-net triangle 02, 01, 11, in Fig. 3, and the pink BB-net triangle 01, 00, 10 are similar and similar to the PS-split sub-triangle with indices 00, 20, 02. Therefore G_{sym}^1 holds with $b(u) = 2 \cos \alpha$. That is, the Greville abscissae satisfy G_{sym}^1 with constant b and the transitions are parameterically C^1 . \square

To obtain a global C^1 function over the Powell-Sabin 6-split, it is then necessary and sufficient to place, for every o , all \mathbf{p}_{ij}^{oab} with $ij \in \{02, 01, 11\}$ into a common (tangent) plane (colored pink in Fig. 3), and, for every triangle oab , all \mathbf{p}_{ij}^{oab} with $ij \in \{01, 00, 10\}$ into a common (tangent) plane (colored green in Fig. 3). For every edge ob , \mathbf{p}_{20}^{ob*} is the average both of \mathbf{p}_{10}^{ob*} and \mathbf{p}_{10}^{o*b} across, or, alternatively, \mathbf{p}_{11}^{ob*} and \mathbf{p}_{11}^{bo*} along the macro-triangle boundary. This leaves free, exactly the choice of value and first derivatives at the vertices of the original triangulation.

We now choose as input the triangulation of an octahedron, see Fig. 3c, with vertices $\pm 12\mathbf{e}_i$, where \mathbf{e}_i are the unit vectors: $\mathbf{e}_i(j) = 0$ for $j \neq i$ and $\mathbf{e}_i(i) = 1$. Since the input triangulation is structurally and geometrically symmetric, any reasonable output surface should preserve the octahedral symmetry, lest relabeling of the input mesh should change the output surface. Moreover, any non-symmetric output can be averaged with its orbit under octahedral symmetry since they use the same reparameterizations $b(u)$. Therefore, failure to construct a symmetric solution implies the non-existence of a non-symmetric solution.

Therefore the pink and green sub-tiles in Fig. 3c must form tangent planes at 00 and 02. The only degree of freedom is the length of $\mathbf{p}_{01} - \mathbf{p}_{02}$, i.e. the extent of the green square. However, regardless of the non-zero extent, all such constructions are non-smooth as Fig. 4 illustrates for a natural choice, and Lemma 4 makes precise. The tangent mismatch occurs along the *vertex-to-center diagonal* with labels 00, 01, 02 that connects the center \mathbf{p}_{00} to the vertex \mathbf{p}_{02} .

Lemma 4. *The octahedron triangulation does not admit a G_{sym}^1 Powell-Sabin surface.*

Proof. Due to symmetry, for the triangulation of the octahedron,

$$\begin{aligned} \mathbf{p}_{00}^{oab} &:= (\mathbf{p}_{01}^{oab} + \mathbf{p}_{01}^{abo} + \mathbf{p}_{01}^{boa})/3, \\ \mathbf{p}_{10}^{oab} &:= (\mathbf{p}_{01}^{oba} + \mathbf{p}_{01}^{boa})/2, \quad \mathbf{p}_{11}^{oab} := (\mathbf{p}_{01}^{oba} + \mathbf{p}_{01}^{obc})/2, \quad \mathbf{p}_{20}^{oab} := (\mathbf{p}_{10}^{oba} + \mathbf{p}_{10}^{obc})/2, \end{aligned}$$

has to hold, as well as

$$\mathbf{p}_{11} - \mathbf{p}_{02} + \mathbf{q}_{11} - \mathbf{q}_{02} = (1 + c_n)(\mathbf{p}_{01} - \mathbf{p}_{02}), \quad c_n := \cos(2\pi/n), \quad (2)$$

$$\mathbf{p}_{10} - \mathbf{p}_{01} + \mathbf{q}_{10} - \mathbf{q}_{01} = (1 - c_3)(\mathbf{p}_{00} - \mathbf{p}_{01}). \quad (3)$$



Figure 4: The Powell-Sabin construction applied to the triangulation of the octahedron results in a non-smooth surface. Two views and right: highlight lines.

where $n = 4$ is the valence at \mathbf{p}_{02} . Since $1 + c_4 = 1 \neq \frac{3}{2} = (1 - c_3)$, Eqs. (2), (3) contradict the existence of a constant β in (1) and G_{sym}^1 can not hold. \square

We note that when $n = 6$, in lieu of the $n = 4$ encountered at the vertices of the octahedron, then $1 + c_n$ and $1 - c_3$ at the endpoints is consistent with $b(0) = b(1) = b(u) = 3/2$ constant. However, a ‘Platonic’ shape with $n = 6$ everywhere corresponds to a flat triangulation where the known smooth piecewise quadratic function is the Powell-Sabin spline.

3. Shape constraints for piecewise quadratic G^1 surfaces of genus other than 1

This section establishes a closed surface whose genus is not 1 requires a nonlinear G^1 reparameterization between some pair of its pieces. Next we argue why we can rule out of consideration constructions that are always asymmetric or always singular. Then Theorem 1 proves that piecewise quadratic surfaces of genus not 1 must have flat neighborhoods or highly oscillating neighborhoods.

Lemma 5. *Let M be a closed compact surface constructed by enforcing (G1) of Lemma 1 between the pieces. If M has genus other than 1 then at least one pair \mathbf{p}, \mathbf{q} has at least one of λ, μ, ν not constant.*

Proof. A G^1 smooth surface of genus g can be cut by $2g$ loops through a common point to yield a one-boundary surface that is homeomorphic to a disk, see e.g. De Verdière and Lazarus (2005); Erickson and Whittlesey (2005). By Observation 1, if λ, μ, ν are constant for all pairs \mathbf{p}, \mathbf{q} satisfying (G1) then the domain of the cut surface can be embedded into \mathbb{R}^2 so that the $2g$ edges, emanating from and ending in the pre-image of the common point, form opening angles that sum to 2π . Since $2\pi = (n - 2)\pi$ must hold for any curvilinear polygon, the polygon must be 4-sided. Interpreted as the fundamental polygon of a compact surface, the surface must be of genus 1, i.e. topologically equivalent to either the torus or the Klein Bottle. In short, λ, μ, ν constant for all pairs \mathbf{p}, \mathbf{q} implies that the surface is of genus 1. This implies the contrapositive statement that, for a G^1 surface of genus not 1, there must be at least one pair with not all λ, μ, ν constant. \square

An alternative argument considers the manifold \tilde{M} of domains joined locally by affine (re)parameterizations $\rho : \mathbf{u} \rightarrow \bar{\mathbf{u}}$ across boundaries. Under this change of variables the Christoffel symbols Γ of any manifold transform (cf. Wikipedia contributors (2025)) by

$$\bar{\Gamma}_{kl}^i = \frac{\partial \bar{\mathbf{u}}^i}{\partial \mathbf{u}^m} \frac{\partial \mathbf{u}^n}{\partial \bar{\mathbf{u}}^k} \frac{\partial \mathbf{u}^p}{\partial \bar{\mathbf{u}}^l} \Gamma_{np}^m + \frac{\partial^2 \mathbf{u}^m}{\partial \bar{\mathbf{u}}^k \partial \bar{\mathbf{u}}^l} \frac{\partial \bar{\mathbf{u}}^i}{\partial \mathbf{u}^m}.$$

Since \tilde{M} has exclusively affine ρ , $\frac{\partial^2 \mathbf{u}^m}{\partial \bar{\mathbf{u}}^k \partial \bar{\mathbf{u}}^l} = 0$ and all second summands vanish. Therefore the assignment $\Gamma_{\nu\sigma}^\mu = 0$ for all transitions of \tilde{M} is permissible. The zero choice implies that the Gauss curvature K is zero. The Gauss Bonnet theorem, $\int_{\tilde{M}} K dA = 2\pi\chi(\tilde{M})$, implies that $0 = \chi(\tilde{M}) = 2 - 2g$, i.e. the genus of \tilde{M} must be 1.

We now focus on a pair of polynomial pieces \mathbf{p}, \mathbf{q} joined G^1 along a common edge so that at least one of λ, μ, ν is not constant. Since the outcome of the surface construction should not depend on the enumeration order of \mathbf{p} and \mathbf{q} and should be symmetric for symmetric designs,

- any reasonable G^1 construction should allow for (not rule out) construction symmetry of the form $\mu = \nu$.

That is, we will not consider constructions that *always* force $\mu \neq \nu$, because such constructions would need to always be asymmetric, also for symmetric data. For such structurally asymmetric constructions, relabeling symmetric input data would yield different surfaces. Analogously, we rule out constructions that *always* enforce $\nu(0) = 0$ or $\nu(1) = 0$, i.e. always yield a singular surface. We will see later that singular quadratic surfaces additionally have flat spots. We can therefore consider a pair \mathbf{p}, \mathbf{q} with λ, μ, ν not all constant so that $\mu = \nu$, and $\nu(0) \neq 0 \neq \nu(1)$. Then the the G_{sym}^1 constraints apply and at the end points of the common boundary, i.e. parameters $u = 0$ and $u = 1$,

$$\begin{bmatrix} b(0)\partial_u \mathbf{q}(0,0) \\ b(1)\partial_u \mathbf{q}(1,0) \end{bmatrix} = \begin{bmatrix} \partial_v \mathbf{p}(0,0) \\ \partial_v \mathbf{p}(1,0) \end{bmatrix} + \begin{bmatrix} \partial_v \mathbf{q}(0,0) \\ \partial_v \mathbf{q}(1,0) \end{bmatrix}, \quad b(0) := \frac{\lambda(0)}{\nu(0)}, \quad b(1) := \frac{\lambda(1)}{\nu(1)}, \quad (4)$$

where $\partial_s := \frac{\partial}{\partial s}$. Since, by assumption, the scalar function $b(\cdot)$ is not constant on the boundary, either $b(0) \neq b(1)$ or we split the boundary, to obtain pieces of \mathbf{p} and \mathbf{q} that join G^1 and so that $b(0) \neq b(1)$. This allows characterizing shape constraints for any smooth quadratic construction with non-constant $b(u)$.

Theorem 1 (shape constraints). *Consider an endpoint \mathbf{e} of a boundary between a pair \mathbf{p}, \mathbf{q} of total degree 2 surface pieces satisfying (G1) with at least one non-constant triple λ, μ, ν with $\mu = \nu$ and $\mu \neq 0$ at \mathbf{e} . Then, at \mathbf{e} , the surface*

- *either has a flat region,*
- or else, and only if the number of patches joining at the vertex is an even $2n$,*
- *an oscillation with n maxima and n minima.*

Proof. Consider two patches \mathbf{p} and \mathbf{q} of total degree 2 that share a boundary curve $\mathbf{p}(u, 0) = \mathbf{q}(u, 0)$. We use the following smoothness characterization, equivalent to (G1), see (Peters, 1990, Lemma 2.ii):

$$0 = \det[\mathbf{q}_u, \mathbf{p}_v, \mathbf{q}_v](u), \quad \mathbf{q}_u(u) := (\partial_u \mathbf{p})(u, 0), \quad \mathbf{p}_v(u) := (\partial_v \mathbf{p})(u, 0), \quad \mathbf{q}_v(u) := (\partial_v \mathbf{q})(u, 0). \quad (5)$$

The determinant polynomial is of degree 3. Equation (5) states that all four BB-coefficients of the determinant must vanish. We abbreviate the un-normalized normal directions at the end points as $\mathbf{n}(0) := \mathbf{q}_u(0) \times \mathbf{p}_v(0)$ and $\mathbf{n}(1) := \mathbf{q}_u(1) \times \mathbf{p}_v(1)$. The first coefficient of the determinant is $\mathbf{n}(0) \cdot \mathbf{q}_v(0) = 0$ and the second (scaled by 3) is

$$\begin{aligned} & \det[\mathbf{q}_u(0), \mathbf{p}_v(0), \mathbf{q}_v(1)] + \det[\mathbf{q}_u(0), \mathbf{p}_v(1), \mathbf{q}_v(0)] + \det[\mathbf{q}_u(1), \mathbf{p}_v(0), \mathbf{q}_v(0)] \\ &= \mathbf{n}(0) \cdot \mathbf{q}_v(1) + \det[\mathbf{q}_u(0), \mathbf{p}_v(1), -\mathbf{p}_v(0) + b(0)\mathbf{q}_u(0)] + \det[\mathbf{q}_u(1), \mathbf{p}_v(0), -\mathbf{p}_v(0) + b(0)\mathbf{q}_u(0)] \\ &= \mathbf{n}(0) \cdot \mathbf{q}_v(1) + \mathbf{n}(0) \cdot \mathbf{p}_v(1) - b(0)\mathbf{n}(0) \cdot \mathbf{q}_u(1) \\ &= \mathbf{n}(0) \cdot (\mathbf{q}_v(1) + \mathbf{p}_v(1) - b(0)\mathbf{q}_u(1)) \\ &= (b(1) - b(0))\mathbf{n}(0) \cdot \mathbf{q}_u(1), \end{aligned}$$

where we use the first equation of (4) in the form: $\partial_v \mathbf{q}(0, 0) = b(0)\partial_u \mathbf{q}(0, 0) - \partial_v \mathbf{p}(0, 0)$ in the expansion and $\partial_v \mathbf{q}(1, 0) + \partial_v \mathbf{p}(1, 0) = b(1)\partial_u \mathbf{q}(1, 0)$ in the last equality. Since, by assumption, $b(1) \neq b(0)$, it holds that $\mathbf{n}(0) \cdot \mathbf{q}_u(1) = 0$. Exchanging $0 \leftrightarrow 1$ to obtain the equation for setting the third coefficient to zero, we therefore need to have

$$\mathbf{n}(0) \cdot \mathbf{q}_u(1) = 0 \text{ and } \mathbf{n}(1) \cdot \mathbf{q}_u(0) = 0.$$

That is, $\mathbf{n}(0)$ is orthogonal to both $\mathbf{q}_u(0)$ and $\mathbf{q}_u(1)$ and $\mathbf{n}(1)$ is orthogonal to both $\mathbf{q}_u(0)$ and $\mathbf{q}_u(1)$.

If $\mathbf{q}_u(0) \times \mathbf{q}_u(1) \neq 0$ then $\mathbf{n}(0)$ and $\mathbf{n}(1)$ are co-linear. Since a quadratic boundary curve cannot have an inflection this implies that the boundary curve $\mathbf{p}(u, 0) = \mathbf{q}(u, 0)$ lies fully in the tangent plane at either end $u \in \{0, 1\}$ of $\mathbf{q}(u, 0)$. Therefore all 2×5 BB-coefficients involved in the G_{sym}^1 join are co-planar. If $\mathbf{q}_u(0) \times \mathbf{q}_u(1) = 0$ then the boundary curve is a straight line and $\mathbf{n}(0) \cdot \mathbf{p}_{uu}(0, 0) = 0$, i.e. the normal component of the second derivative is zero. Case (i): assume that a neighbor boundary curve \mathbf{f} emanating from $\mathbf{p}(0, 0)$ is not straight, i.e. $\mathbf{f}_0(0) \times \mathbf{f}_u(1) \neq 0$. Then, by the above paragraph, all 2×5 BB-coefficients involved in the G_{sym}^1 join are co-planar. Therefore the normal

component of the mixed derivative $\mathbf{n}(0) \cdot (\partial_u \partial_v \mathbf{p})(0, 0) = 0$ and all BB-coefficients involved in the G_{sym}^1 join across $\mathbf{p}(u, 0) = \mathbf{q}(u, 0)$ are co-planar. In summary, if there is a single boundary curve emanating from $\mathbf{p}(0, 0)$ such that $\mathbf{f}_u(0) \times \mathbf{f}_u(1) \neq 0$ then the whole neighborhood is co-planar (flat).

Case (ii): assume $\mathbf{f}_u(0) \times \mathbf{f}_u(1) = 0$ for all n curves emanating from $\mathbf{p}(0, 0)$. Differentiating the relation G_{sym}^1 in the boundary direction u and retaining only the normal component yields, cf. the vertex enclosure theorem (Peters, 1990, Lemma 3.4), only the mixed derivative terms:

$$0 = \mathbf{n}(0) \cdot ((\partial_u \partial_v \mathbf{p})(0, 0) + (\partial_u \partial_v \mathbf{q})(0, 0)).$$

If we express the mixed derivative in terms of differences of BB-coefficients $\mathbf{p}_{00} - \mathbf{p}_{10} - \mathbf{p}_{01} + \mathbf{p}_{11}$, where $\mathbf{p}_{10} - \mathbf{p}_{00}$ and $\mathbf{p}_{01} - \mathbf{p}_{00}$ are the tangent directions at $\mathbf{p}_{00} = \mathbf{p}(0, 0)$, then $\mathbf{n}(0) \cdot \mathbf{p}_{11} = -\mathbf{n}(0) \cdot \mathbf{q}_{11}$. Therefore, if an odd number of quadratic patches meet at $\mathbf{p}(0, 0)$ or if the surface is convex, all BB-coefficients of the quadratics with must be co-planar. If the surface is not flat, the number must be even and $\mathbf{n}(0) \cdot \mathbf{p}_{11} = -\mathbf{n}(0) \cdot \mathbf{q}_{11}$. This relation forces $2n$ alternations of sign, i.e. the surface oscillates with exactly n minima and n maxima. \square

In most modeling situations neither forced flat regions nor oscillations are desirable. Nevertheless, Theorem 1 leaves these options to be explored.

4. Special quadratic surface constructions

Theorem 1 still allows for quadratic G^1 free-form surface constructions – by side-stepping the assumptions or abiding by the constraints of Theorem 1 and abiding by the shape restrictions.

Constructions leaving out cut points. One can choose a domain of the expected topological genus, flattening the fundamental domain, and then construct Powell-Sabin splines on the flattened domain. Leaving out one, or up to $2g-2$ cut point neighborhoods, He et al. (2005), and more recently Capouellez et al. (2023), have constructed Powell-Sabin splines of total degree 2 on the flattened triangulation. Gu et al. (2006) suggest using degree 2 simplex splines instead. Since these approaches do not succeed in covering the cut points with a smooth surface consisting of polynomial pieces of total degree 2, they do not address the questions of the Introduction.

Constructions using non-standard domains. If one does not insist on parameterizing each degree 2 surface piece over the assumed straight-edged unit triangles in the Euclidean plane domain, polynomial free-form surfaces of total degree 2 can be constructed. Trivially, as a function on the sphere as domain, the sphere itself is just the identity. As a second example, Farin et al. (1987) reproduce the sphere by eight non-degenerate rational pieces of total degree 2 in BB-form:

$$\frac{\mathbf{q}}{q}(u, v) := \frac{\sum_{i+j+k=2} w_{ijk} \mathbf{p}_{ij} B_{ijk}(u, v)}{\sum_{i+j+k=2} w_{ijk} B_{ijk}(u, v)}, \quad \mathbf{q}_{ijk} := w_{ijk} \mathbf{p}_{ij} \in \mathbb{R}^3, \quad (6)$$

essentially piecemeal reproducing the stereographic projection $(2u/(1+u^2+v^2), 2v/(1+u^2+v^2), (1-u^2-v^2)/(1+u^2+v^2))$. Each piece is defined over a flat triangle with two straight and one quadratically curved edge. Of course, if this curved triangle is expressed as the rational quadratic image of a straight-edged triangle, the composed map is of degree 4. Orbifold splines Wallner and Pottmann (1997) and RAGS Beccari et al. (2014); Beccari and Neamtu (2016); Beccari and Prautzsch (2022) define splines on the hyperbolic plane, where the corner angle sum argument of Lemma 5 no longer holds. In order to re-use techniques from the planar case, the hyperbolic plane can be represented via its planar Klein or Poincaré models where the domain is covered by a fundamental polygon, with straight edges for the Klein model or curved ones for the Poincaré model. An alternative approach, generalizing Maes and Bultheel (2007) by mapping projective spaces $\mathbf{P}^2 \rightarrow \mathbf{P}^3$, has been developed by Prautzsch (2022).

Constructions restricted to domains of genus 1. Besides the PS spline over general flat triangulations, the ZP spline of Zwart (1973) is a piecewise quadratic on a quincunx grid with directions $e_1, e_2, e_1 - e_1, e_1 + e_2$, see Fig. 1 a. Therefore G_{sym}^1 holds with $b(u) = 1$ and $b(u) = 0$. Since the ZP spline is a 4-direction box-spline shifted on the regular integer grid, see e.g. De Boor et al. (2013); Kim and Peters (2024), the genus of the surface is restricted to 1.

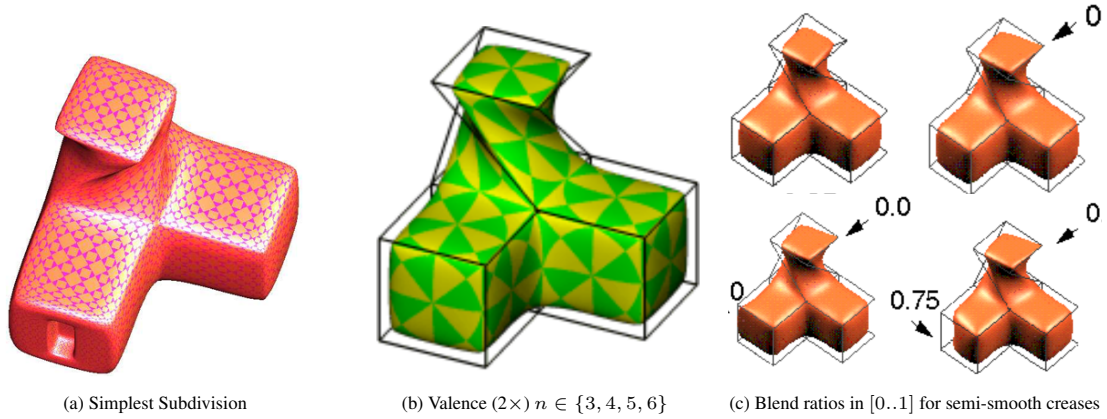


Figure 5: (a) Degree 2 Simplest Subdivision [Peters and Reif \(1997\)](#). (b,c) Quadratic-cubic C^1 free-form surface splines with vertices of valence $(2 \times) 3, 4, 5, 6$ (c) with blend ratios to generate semi-smooth edges and vertices, or even interpolate edges or vertices [Peters \(1995\)](#).

Constructions using infinitely many pieces. The simplest subdivision [Peters and Reif \(1997\)](#) generalizes the ZP spline to free-form surfaces of arbitrary genus, at the cost of generating an infinite sequence of contracting surface rings of total degree 2 and with the ZP layout, see Fig. 5 a. The resulting piecewise quadratic subdivision surface is C^1 , see e.g. [Peters and Reif \(2008\)](#).

Constructions with a singular parameterization. A singular parameterization is proposed as an exercise in Ch 12.5 of [Prautzsch et al. \(2002\)](#). However, this approach leads not just to a singularity but, by Theorem 1, additionally to flatness, since oscillation of the singularly parameterized quadratic is not possible.

Constructions with additional degree 3 pieces. By combining the total degree 2 ZP element with polynomial pieces of total degree 3 at non-4-valent vertices [Peters \(1995\)](#), one can choose a linear β in (1) and generate non-singular total degree quadratic-cubic free-form surfaces of unrestricted genus, see e.g. Fig. 5 b,c. By parameterizing the built-in switch from an initial general control net to the ZP-compatible (vertex-valence 4) control net, this free-form spline can have semi-smooth creases. Specifically, one can set scalars, called blend ratios, in $(0..1)$, and obtain sharp creases for ratios 0 or 1 where 1 results in interpolation of edges or vertices, see Fig. 6 c.

Constructions enforcing flat regions. Considering the first case of Theorem 1, we exhibit a construction that yields everywhere quadratic, G^1 smooth free-form surfaces that are not restricted in genus or local connectivity, nor singularly parameterized – but are flat in every neighborhood of vertices of valence $2n$, $n > 4$. The required nonlinear change of variables is placed in the flat parts. Fig. 6 a shows such a G^1 quadratic free-form surface, with flat regions where $2n > 8$ pieces meet. Fig. 6 c,d,e illustrate the steps of the

Algorithm for constructing G^1 surfaces entirely from quadratic pieces at the cost of flat spots.

1. The initial mesh is refined by at most one step of [Catmull and Clark \(1978\)](#) and two steps of [Doo and Sabin \(1978\)](#), as illustrated in Fig. 6 c (for an $n = 6$ -valent vertex of the quad mesh that is delineated by solid lines in Fig. 5 b). This yields an ever finer mesh with nodes marked respectively \bullet , \cdot , \circ .
2. At the finest level, nearest to the center (note: the central point not included since Doo-Sabin is a ‘dual’ subdivision algorithm), two layers (displayed in Fig. 6 c as \bullet rather than \cdot) are projected into a common plane. The projected points are shown again in the zoom of Fig. 6 d as \circ .
3. This finest level is interpreted as a ZP control net, see Fig. 1.
4. Convert the ZP elements to their BB-form of degree 2. This yields the BB-coefficients marked $+$, respectively \blacksquare for the three innermost layers.

We observe:

- The BB-coefficients marked \blacksquare are co-planar.
- The $2n$ quadratic pieces of the first layer, i.e. touching the center (see the piece of the kite-like shape touching the center in Fig. 6 d) lie in one plane.

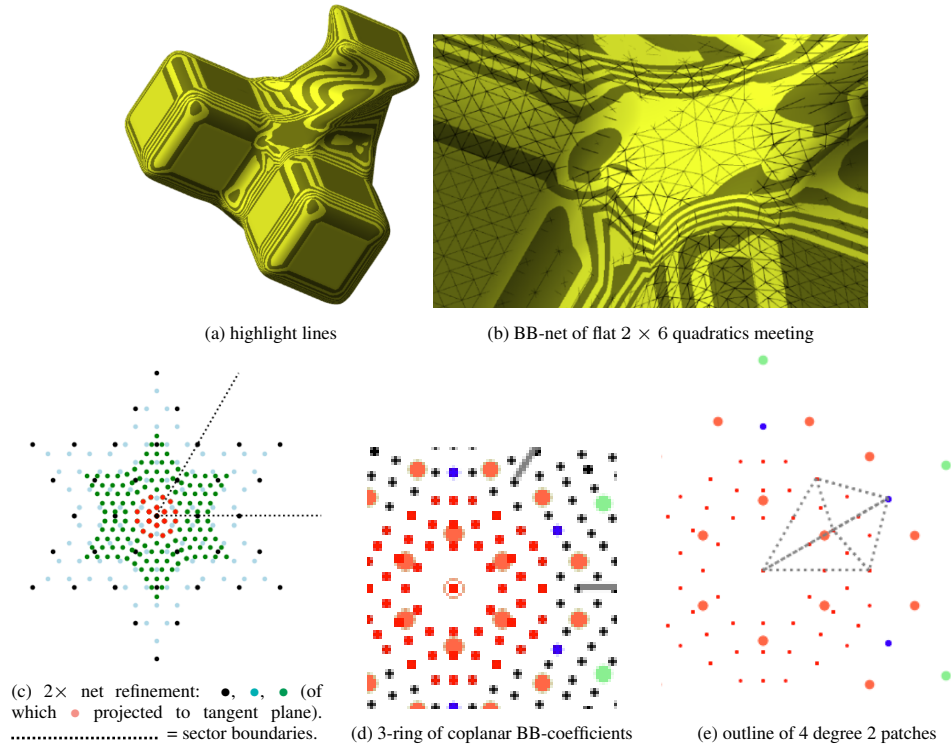


Figure 6: Quadratic free-form surface construction with flat regions. (a) The highlight line distribution on a G_{sym}^1 free-form surface of total degree 2 with flat regions where $2n > 8$ quadratics join. (b) Zoom on the flat region an BB-net where $2n = 12$ quadratics join at one point. (c) One Catmull-Clark refinement yields \bullet , a second Doo-Sabin refinement yields \cdot , and a second Doo-Sabin refinement yields \cdot and \cdot , of which the \cdot points are projected into a common plane. (The Doo-Sabin nets do not include a central point). (d) The enlarged ZP-points \cdot are coplanar. Therefore the BB-coefficients $+$ and \cdot forming the innermost three layers are coplanar. (e) The outline of four quadratics that share an enabling configuration are dashed (compare to Fig. 2 b). The two patches closer to the center, and hence the innermost $2 \times n$ patches, are flat. Of the other two patches, only the furthest BB-coefficient \cdot is not in the tangent plane of the central point, so the outer two pieces can be curved.

- In the next, the second layer of quadratics, only the furthest BB-coefficient, marked ■, does not lie in the central (tangent) plane.

That is, this second layer of total degree 2 patches can be curved. For the first, central layer, G_{sym}^1 does not hold. But the surface is geometrically C^1 since the quadratic pieces of the central layer completely lie in the tangent plane. Note that this flat construction differs from the flat spots due to cone degeneracy in (Capouellez et al., 2023, Suppl 1) and Ch 12.5 of Prautzsch et al. (2002).

To mitigate the flat spots, a construction could add, normal to the flat region, a local piecewise quadratic q that vanishes towards the boundary of the flat region. This variant is not explored since the goal is to characterize minimal degree for smooth surfaces and the approach is both more complex than introducing total degree 3 surface pieces and unlikely to result in design-level surfaces.

Constructions enforcing saddles of high order. For higher-order saddles, the alternative to flatness in Theorem 1, namely n minima and n maxima, seems at first relevant. However, the algorithm constructs $2n$ quadratics at the original points, so that the frequency is twice of what one would want for a saddle indicated by the original quad mesh: for the monkey saddle in Fig. 6 the 12 quadratics would have to yield 6 maxima and minima, rather than the appropriate 3 maxima and minima.

Constructions by restriction to a manifold. One can define surfaces over a manifold $\mathcal{M} \in \mathbb{R}^3$ by constructing a function $f : \mathbb{R}^3 \rightarrow \mathbb{R}$ whose domain covers the manifold and by restriction f to \mathcal{M} . Alfeld et al. (1996a) expressed spherical harmonics as restrictions of homogeneous (harmonic) trivariate polynomials to the unit sphere (see also Alfeld et al. (1996b) and Liu and Schumaker (1996)).

Constructions as level sets of trivariate quadratics. One can construct quadric surfaces as zero sets of trivariate quadratic polynomials over tetrahedra or other trivariate domains. The resulting implicit surface is a quadric and quadrics can be parameterized as rational quadratics. For composite surfaces, one needs to first build a simplicial complex on which to create the trivariate C^1 structure. For example, to construct a sphere, as the joint zero level set of 8 trivariate homogeneous polynomial pieces of total degree 2 on 8 tetrahedra that symmetrically partition an octahedral solid. For the trivariate quadratics to join C^1 , all BB-coefficients other than those at the vertices need to be zero. That is

$$\text{for } i, j, k \in \mathbb{N}_0, i + j + k = 2 : \mathbf{p}_{ijk}^{abc} = \begin{cases} 1 & \text{if } i = 2 \text{ or } j = 2 \text{ or } k = 2, \\ 0 & \text{else.} \end{cases}$$

Dahmen (1989) and Guo (1993) provide an algebraic construction based on a trivariate Powell-Sabin split that requires a global transversal system. Bangert and Prautzsch (1999) provide a geometric construction that generalizes the algebraic constructions.

5. Conclusion

Since the least-degree, smooth, piecewise polynomial Powell-Sabin construction fails to generate G^1 general free-form surfaces, already over the triangles of an octahedron, this paper asked whether this failure is just an artifact of the particular construction, or whether there exists a more fundamental lower bound on the polynomial degree. Theorem 1 derived fundamental restrictions on the shape of smoothly-joined quadratics. We listed a number of ways that the assumptions of Theorem 1 can and have been circumvented. And we gave an Algorithm in case that shape restrictions can be accepted, namely flat regions at points where more than eight quadratics meet. In short: using only quadratic pieces, and ruling out undesirable always singular or always asymmetric (hence for symmetric data labeling dependent) constructions, there is no approach that allows modeling G^1 surfaces of genus other than 1 – except for the intentional introduction of flat spots or high oscillations. A construction is presented that yields everywhere smooth quadratic surfaces at the cost of flat spots.

Acknowledgements Xiaofeng Gu pointed the first author to the alternative argument following Lemma 5.

References

- Alfeld, P., Neamtu, M., Schumaker, L.L., 1996a. Bernstein-Bézier polynomials on spheres and sphere-like surfaces. *Computer Aided Geometric Design* 13, 333–349.
- Alfeld, P., Neamtu, M., Schumaker, L.L., 1996b. Fitting scattered data on sphere-like surfaces using spherical splines. *Journal of Computational and Applied Mathematics* 73, 5–43.
- Bangert, C., Prautzsch, H., 1999. Quadric splines. *Computer Aided Geometric Design* 16, 497–515.
- Bastl, B., Jüttler, B., Kosinka, J., Lávička, M., 2008. Computing exact rational offsets of quadratic triangular Bézier surface patches. *Computer-Aided Design* 40, 197–209.
- Beccari, C.V., Gonsor, D.E., Neamtu, M., 2014. RAGS: Rational geometric splines for surfaces of arbitrary topology. *Computer Aided Geometric Design* 31, 97–110.
- Beccari, C.V., Neamtu, M., 2016. On constructing RAGS via homogeneous splines. *Computer Aided Geometric Design* 43, 109–122.
- Beccari, C.V., Prautzsch, H., 2022. Quadrilateral orbifold splines, in: *Geometric Challenges in Isogeometric Analysis*. Springer, pp. 1–18.
- Beirão da Veiga, L., Hughes, T.J.R., Kiendl, J., Lovadina, C., Niiranen, J., Reali, A., Speleers, H., 2015. A locking-free model for Reissner-Mindlin plates: Analysis and isogeometric implementation via NURBS and triangular NURPS. *Math. Models Methods Appl. Sci.* 25, 1519–1551.
- de Boor, C., 1987. B-form basics, in: Farin, G. (Ed.), *Geometric Modeling: Algorithms and New Trends*, SIAM, pp. 131–148.
- Capouellez, R., Dai, J., Hertzmann, A., Zorin, D., 2023. Algebraic smooth occluding contours, in: *ACM SIGGRAPH 2023 Conference Proceedings*, pp. 1–10.
- Catmull, E., Clark, J., 1978. Recursively generated B-spline surfaces on arbitrary topological meshes. *Computer-Aided Design* 10, 350–355.
- Cohen, E., Lyche, T., Riesenfeld, R.F., 2013. A B-spline-like basis for the Powell-Sabin 12-split based on simplex splines. *Mathematics of Computation*, 1667–1707.
- Dahmen, W., 1989. Smooth piecewise quadric surfaces, in: *Mathematical methods in computer aided geometric design*. Elsevier, pp. 181–193.
- De Boor, C., Höllig, K., Riemenschneider, S., 2013. Box splines. volume 98. Springer Science & Business Media.
- De Verdière, É.C., Lazarus, F., 2005. Optimal system of loops on an orientable surface. *Discrete & Computational Geometry* 33, 507–534.
- DeRose, T.D., 1990. Necessary and sufficient conditions for tangent plane continuity of Bézier surfaces. *Comp Aid Geom Design* 7, 165–179.
- Dierckx, P., 1997. On calculating normalized Powell-Sabin B-splines. *Computer Aided Geometric Design* 15, 61–78.
- Dierckx, P., Van Leemput, S., Vermeire, T., 1992. Algorithms for surface fitting using Powell-Sabin splines. *IMA Journal of numerical analysis* 12, 271–299.
- Doo, D., Sabin, M., 1978. Behaviour of recursive division surfaces near extraordinary points. *Computer-Aided Design* 10, 356–360.
- Erickson, J., Whittlesey, K., 2005. Greedy optimal homotopy and homology generators, in: *SODA*, pp. 1038–1046.
- Farin, G., 1988. *Curves and Surfaces for Computer Aided Geometric Design: A Practical Guide*. Academic Press.
- Farin, G., Piper, B., Worsey, A.J., 1987. The octant of a sphere as a non-degenerate triangular Bézier patch. *Computer Aided Geometric Design* 4, 329–332.
- Gu, X., He, Y., Qin, H., 2006. Manifold splines. *Graph. Model* 68, 237–254.
- Guo, B., 1993. Representation of arbitrary shapes using implicit quadrics. *The Visual Computer* 9, 267–277.
- He, Y., Jin, M., Gu, X., Qin, H., 2005. A C^1 globally interpolatory spline of arbitrary topology, in: *International Workshop on Variational, Geometric, and Level Set Methods in Computer Vision*, Springer, pp. 295–306.
- Kim, M., Peters, J., 2024. A practical box spline compendium. *Applied Mathematics and Computation* 464, 128376.
- Liu, X., Schumaker, L.L., 1996. Hybrid Bézier patches on sphere-like surfaces. *Journal of computational and applied Mathematics* 73, 157–172.
- Lyche, T., Muntingh, G., 2019. B-spline-like bases for C^2 cubics on the Powell-Sabin 12-split. *The SMAI Journal of computational mathematics* 5, 129–159.
- Maes, J., Bultheel, A., 2007. Modeling sphere-like manifolds with spherical Powell-Sabin B-splines. *Computer aided geometric design* 24, 79–89.
- Manni, C., Sablonniere, P., 2007. Quadratic spline quasi-interpolants on Powell-Sabin partitions. *Advances in Computational Mathematics* 26, 283–304.
- Peters, J., 1990. Fitting smooth parametric surfaces to 3D data. Ph.D. thesis. University of Wisconsin. PhD thesis; see also CMS Technical Report 91-2.
- Peters, J., 1995. C^1 -Surface Splines. *SIAM Journal on Numerical Analysis* 32, 645–666.
- Peters, J., Reif, U., 1997. The simplest subdivision scheme for smoothing polyhedra. *ACM Transactions on Graphics* 16, 420–431.
- Peters, J., Reif, U., 2008. *Subdivision Surfaces*. volume 3 of *Geometry and Computing*. Springer-Verlag, New York.
- Powell, M.J., Sabin, M.A., 1977. Piecewise quadratic approximations on triangles. *ACM Transactions on Mathematical Software (TOMS)* 3, 316–325.
- Prautzsch, H., 2022. Rational spline manifolds. URL: https://events.unibo.it/file/book_SMART_2022. SMART 2022, Rimini, Italy.
- Prautzsch, H., Boehm, W., Paluszny, M., 2002. Bézier and B-spline techniques. volume 6. Springer.
- Speleers, H., Dierckx, P., Vandewalle, S., 2006. Local subdivision of Powell-Sabin splines. *Computer aided geometric design* 23, 446–462.
- Speleers, H., Dierckx, P., Vandewalle, S., 2007. Weight control for modelling with NURPS surfaces. *Comput. Aided Geom. Design* 24, 179–186.
- Speleers, H., Manni, C., Pelosi, F., 2013. From NURBS to NURPS geometries. *Comput. Methods Appl. Mech. Engrg.* 255, 238–254.
- Speleers, H., Manni, C., Pelosi, F., Sampoli, M.L., 2012. Isogeometric analysis with Powell-Sabin splines for advection-diffusion-reaction problems. *Comput. Methods Appl. Mech. Engrg.* 221–222, 132–148.
- Wallner, J., Pottmann, H., 1997. Spline orbifolds. *Curves and Surfaces with Applications in CAGD*, 445–464.
- Wikipedia contributors, 2025. Christoffel symbols. URL: https://en.wikipedia.org/wiki/Christoffel_symbols. [Online; accessed 03-March-2025].
- Windmolders, J., Dierckx, P., 1999. From PS-splines to NURPS, in: Cohen, A., Rabut, C. (Eds.), *Proceedings of Curve and Surface Fitting*, Vanderbilt University Press, Saint Malo. pp. 45–54.

- 348 Windmolders, J., Dierckx, P., 2000. NURPS for special effects and quadrics, in: Lyche, T., Schumaker, L. (Eds.), Proceedings of Mathematical
349 Methods for Curves and Surfaces, Vanderbilt University Press, Oslo. pp. 527–534.
- 350 Zwart, P.B., 1973. Multivariate splines with nondegenerate partitions. SIAM Journal on Numerical Analysis 10, 665–673.